

PAPER • OPEN ACCESS

# Wavelet Processing of Continuous Scanning Laser Doppler Vibrometry data in Non-Destructive Testing

To cite this article: P Chiariotti *et al* 2015 *J. Phys.: Conf. Ser.* **658** 012001

View the [article online](#) for updates and enhancements.

## Related content

- [Performance analysis of continuous tracking laser Doppler vibrometry applied to rotating structures in coast-down](#)  
M Martarelli and P Castellini
- [Vibration measurements using continuous scanning laser Doppler vibrometry: theoretical velocity sensitivity analysis with applications](#)  
B J Halkon and S J Rothberg
- [Laser Doppler vibrometry on rotating structures in coast-down: resonance frequencies and operational deflection shape characterization](#)  
M Martarelli, P Castellini, C Santolini *et al.*

## Recent citations

- [P. Chiariotti \*et al\*](#)



**240th ECS Meeting** ORLANDO, FL

Orange County Convention Center Oct 10-14, 2021



Abstract submission due: April 9

**SUBMIT NOW**

# Wavelet Processing of Continuous Scanning Laser Doppler Vibrometry data in Non-Destructive Testing

P Chiariotti<sup>1\*</sup>, G M Revel<sup>1</sup>, M Martarelli<sup>2</sup>

<sup>1</sup>Università Politecnica delle Marche, via Brecce Bianche, 60131 Ancona, Italy

<sup>2</sup>Università degli Studi e-Campus, via Isimbardi, Novedrate (CO), Italy

E-mail: p.chiariotti@univpm.it

**Abstract.** The present paper proposes a novel non-destructive testing procedure based on the exploitation of the simultaneous time and spatial sampling provided by Continuous Scanning Laser Doppler Vibrometry (CSLDV) and the feature extraction capabilities of wavelet-based processing. Two criteria for selecting in an objective way the mother-wavelet to be used in the decomposition procedure, the Relative Wavelet Energy and Energy to Shannon Entropy Ratio, are compared in terms of capability of best locating the damage. The paper demonstrates the applicability of the procedure for the identification of superficial and in-depth defects in simulated and real test cases when an area scan is performed over the test sample. The method shows promising results, since defects are identified in different severity conditions.

## 1. Introduction

Scientists and engineers all around the world have always been interested in damage detection and location since this is a natural step for a proper condition assessment of structures. Laser Doppler Vibrometry (LDV) has become a well-established technique for non-intrusive vibration measurements. Its potentials are directly related to the wide application fields it has been applied in [1], which go from vibroacoustics [2, 3] to biomedical applications [4]. Several attempts have been made for developing fast and reliable methods wherein LDV is targeted to Structural Health Assessment. An example of such is reported in the work of Castellini et al. [5]. Among the different approaches proposed, it is now well-understood that the presence of damages that modify the modal behaviour of the structure under analysis can be assessed by LDV, both in Discrete (SLDV) and Continuous Scanning (CSLDV) approach.

Stanbridge et al. [6] introduced the Continuous Scanning Laser Doppler Vibrometry (CSLDV) method as an alternative to conventional Scanning Laser Doppler Vibrometry (SLDV). Using CSLDV the Operational Deflection Shapes (ODSs) of a structure can be recovered from a single time history acquired by the Laser Doppler Vibrometer (LDV) while the laser beam scans, in a continuous way, all over the vibrating surface. With respect to Discrete Scanning Laser Doppler Vibrometry, CSLDV presents the following advantages:

- extremely high spatial resolution,
- compact data structure (e.g. a single time history contains both time and spatial information),
- limited duration of the experiment (e.g. acquisition time only depends on the required frequency resolution).

These characteristics have made it possible to use CSLDV for different applications with respect to Experimental Modal Analysis (EMA) and vibration analysis. An example for machinery noise control problems is reported in [7].



When using CSLDV to perform a vibration measurement, the time history appears as an amplitude-modulated signal whose modulation is due to the Operational Deflection Shapes excited during the experiment. This particular aspect makes CSLDV extremely suitable also for damage detection in structural health assessment tests. In 1997 Stanbridge et al. [8] and later on in 2000 Khan et al. [9] demonstrated the effectiveness of using CSLDV for detecting cracks when the crack produces a localized mode shape discontinuity. The approach proposed by Khan et al. consisted in applying a standard demodulation technique, namely multiplying the digitized CSLDV signal, point by point, by a sine wave at the excitation frequency, and passing the result through a low-pass filter. However, such approach presents some drawbacks. Indeed, the choice of the low pass-filter cut-off frequency might seriously affect the possibility of locating a discontinuity in the mode shape; moreover, the use of a demodulation approach implies several trials in order to identify the best-case scenario that is able to enhance the defect. This happens, for instance, when the defect is located on a nodal line for certain mode shapes: demodulation cannot recover the presence of the defect.

Wavelet processing has also been intensively investigated in the last decade for structural health assessment [10, 11, 12]. Some papers that report the use of wavelet processing on mode shapes extracted by SLDV are also present in literature, as the work of Cao et al. [13]. Conventional Discrete Scanning Vibrometry implies the measurement of several vibration points distributed all over the surface. This makes the efficiency of the wavelet processing in extracting the damage information (either from the modal curvature or from a discontinuity in the mode shape) strongly dependent on the dimension of the damage with respect to the spatial sampling used in the experiment. CSLDV overcomes these limits, since it provides a single time history that inherently contains the ODSs information with an almost infinite spatial resolution.

Chiariotti et al. proposed a novel approach that exploits Wavelet-domain processing to extract features related to the damage in the CSLDV signal [14]. This paper aims at presenting an evolution of the approach described in [14], by proposing two objective approaches for selecting the mother-wavelet and presenting some preliminary results of the method on a real test case. Moreover, the focus is on the area scan testing procedure: indeed, such approach represents the only testing solution to be adopted in real test cases, where defects location is never known a-priori.

The paper is organized as follows: Section 2 presents the Damage Detection procedure proposed; Section 3 provides a description of the virtual experiment used to test the procedure on superficial defects and results obtained on different crack scenarios; an application of the approach to a sub-surface damage is presented in Section 4. Section 5 reports results from a real test case. The main conclusions are summarized in Section 6.

## **2. CSLDV-Wavelet based Damage Detection Procedure**

This paper presents a methodology for jointly exploiting CSLDV and wavelet-processing for defect identification. The method can be exploited on both superficial cracks and on sub-surface defects. An example of the latter is presented in Section 4.

A vibration signal acquired by CSLDV is amplitude-modulated by the ODSs excited during the vibration test. Since the laser spot continuously scans the surface of the test specimen, the possibility of passing on a damaged area is highly realistic. For instance, the presence of a crack can introduce discontinuities on certain mode shapes of the structure, and therefore the modulating signal will reflect this discontinuity as well.

If dealing with superficial damages as cracks, the discontinuity in the mode shape will also introduce further complex phenomena linked to the interaction of the laser light with the defect edges. Diffraction, speckle noise in the optical signal coming back to the detector active area and eventually signal drop-outs (depending on the extension of the crack in the scan direction) are examples of such phenomena. Their impact is stronger the more relevant is the discontinuity introduced.

Sub-surface defects either might induce local distortions of mode shapes excited or might introduce local modes. In both cases the amplitude modulation phenomenon produced by the vibrating structure

on the CSLDV signal will carry such distortions. A proper processing can therefore reveal this information and thus can help in identifying the damage location.

Speckle noise, which naturally affects CSLDV [15], has also to be taken into account. However, while the latter is periodic in nature and strongly related to the scan frequency, the phenomena related to light-defect interaction, e.g. for superficial damages, are still periodic but dependent on the transits of the laser spot over the defect.

Wavelet-processing is the best candidate for enhancing these discontinuities, which are introduced by the presence of a damage, in the signal and for localizing them in time domain. Since in CSLDV time and space are related by the signals the laser Doppler vibrometer mirrors are driven with, identify discontinuities in the time history analysed is equal to spatially-localize the damage on the structure under test. The approach is also less sensitive to measurement noise with respect to standard demodulation, since this noise, which is generally Gaussian in nature, is uniformly spread throughout the wavelet space.

The main issue in applying a wavelet-processing consists in choosing the mother wavelet. Literature divides approaching for tackling this issue in two main clusters: qualitative approaches and quantitative approaches. In qualitative approaches, mother-wavelet selection is mainly based on the similarity between the wavelet and the signal. Normally shape matching by visual inspection is the commonest criterion to pick up the right wavelet. However, visually matching the shape of the feature that has to be extracted from the signal and the shape of the wavelet is difficult. Among quantitative approaches the Minimum Description Length (MDL) criterion [16], the Energy to Shannon Entropy Ratio [17] and the variance of the continuous wavelet coefficients [18] are examples of used criteria. A valid literature survey on mother-wavelet selection approaches can be found in the work of Ngui et al. [19].

The Relative Wavelet Energy and Energy to Shannon Entropy Ratio are compared as mother-wavelet selection criteria in the damage detection procedure presented in this paper, even though both criteria were initially developed for Continuous Wavelet Transform (CWT) [20].

The Relative Wavelet Energy (RWE) is defined as the ratio of the Energy at each resolution level and the total energy (1)

$$p_n = \frac{E(n)}{E_{tot}} \quad (1)$$

where the Energy at each resolution level,  $E(n)$ , is defined as reported in (2)

$$E(n) = \sum_{i=1}^m |C_{n,i}|^2 \quad (2)$$

In (2),  $m$  represents the number of wavelet coefficients, and  $C_{n,i}$  the wavelet coefficient at the  $n^{th}$  decomposition node. The total Energy is then estimated as the sum of the energy at each resolution level over all the decomposition nodes (3).

$$E_{tot} = \sum_n E(n) \quad (3)$$

RWE gives information about relative energy with associated frequency bands and can detect the degree of similarity between segments of a signal.

The mother-wavelet is a base wavelet that can extract the maximum amount of energy of a signal while minimizing the Shannon Entropy of the corresponding wavelet coefficients. The Energy to Shannon Entropy Ratio (ESER) aims at fulfilling this criterion, being defined as (4).

$$\zeta_n = \frac{E(n)}{S_{entropy}(n)} \quad (4)$$

In (4),  $E(n)$  represents the energy content at each node of the decomposition tree and refers to (2), while the Shannon Entropy follows the definition reported in (5).

$$S_{entropy}(n) = -\sum_{i=1}^m p_i \log_2 p_i \quad (5)$$

In (5),  $p_i$  represents the probability distribution of the wavelet coefficients, defined as

$$p_i = \frac{|C_{n,i}|^2}{E(n)} \quad (6)$$

The summation of  $p_i$  over the number of wavelet coefficients  $m$  must equal 1, and in case  $p_i=0$  for some  $i$  the full term  $p_i \log_2 p_i$  is considered equal to 0.

Once the original signal is decomposed by wavelet-processing a threshold has to be defined in order to localize discontinuities in the decomposed signal. The authors propose to calculate the threshold ( $t$ ) as the product of Stein's Unbiased Estimate of Risk (SURE) [21] criterion threshold and the RMS (Root Mean Square) of the wavelet-decomposed signal:

$$t = \sqrt{\frac{1}{K} \sum_{k=1}^K x_n(k)^2} \cdot \sqrt{2 \ln \left( \frac{K \ln K}{\ln 2} \right)} \quad (7)$$

where:

- $x_n(k)$ : velocity signal at the  $n^{th}$  decomposition node;
- $K$ : number of samples of the decomposed velocity signal;
- $\ln$ : natural logarithm.

### 3. Application of the method on a superficial defect

The approach was tested on a simulated test case representing a steel plate with several crack scenarios, as reported in Figure 1. Crack scenario I refers to a through-depth damage.

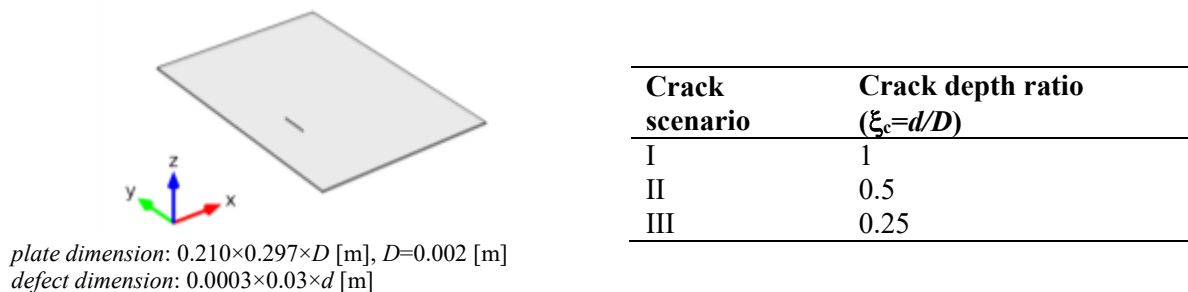


**Figure 1** Geometrical model and crack scenarios used in damage detection tests

In order to synthesize the CSLDV signal, a FEA (Finite Element Analysis) of the steel plate (free-free boundary condition) was performed at first. Such analysis made it possible to extract the mass-normalized mode shapes of the structure. Three main modes, each involving the crack in a different way, were selected for the analysis.

These modes, ranging from 1.1kHz to 2.1kHz, were selected in order to test the influence of the shape with respect to the crack position/orientation (Figure 2). Natural frequencies of each mode according to the different crack scenarios are reported in Table 1.

**Table 1** Natural frequencies of mode shapes used for synthesizing CSLDV signal

Crack to Mode relative position	Frequency [Hz]		
	$\xi_c=1$	$\xi_c=0.5$	$\xi_c=0.25$
Crack on antinode	1105	1106.5	1106.9
Crack on a node	1203	1204.2	1204.4
Crack on a generic position	2083	2090	2091.4

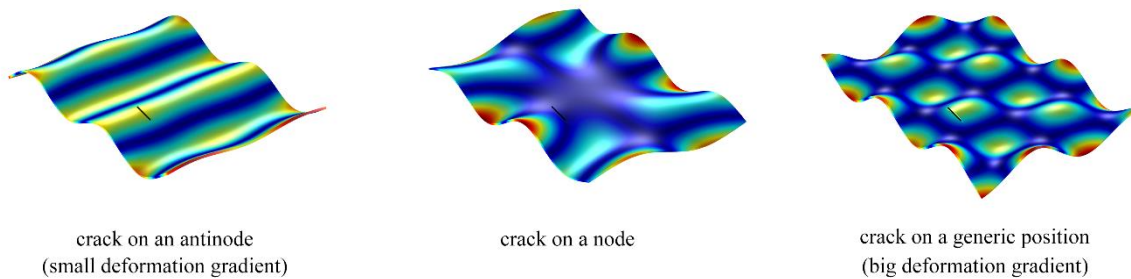


**Figure 2** Mode shapes selected for synthesizing the CSLDV signal

The shapes to be used as amplitude-modulating functions for the vibration signal were extracted on a simulated scan path reproducing the laser spot scanning the surface. Crack location is never known a priori in a real case scenario. For such reason it is important to perform a 2D scan. An area scan obtained by creating the Lissajous pattern (8) reported in Figure 3 was used to build the synthesized CSLDV signal discussed in this section.

$$\begin{cases} x = A_x \sin(2\pi f_x t + \Phi_x) \\ y = A_y \sin(2\pi f_y t + \Phi_y) \end{cases} \quad (8)$$

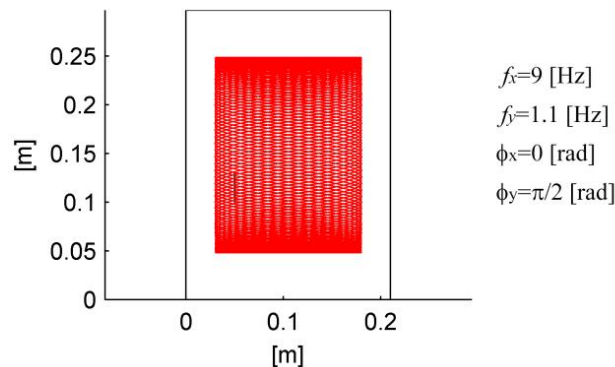


**Figure 3** Lissajous pattern used to virtually perform an area scan on the test plate

The digital signal was generated simulating a sampling frequency ( $f_s$ ) of 100kHz and a recording time ( $T$ ) of 20s. Since it is expected that the laser signal is affected by light-crack interaction, this event was reproduced, to a first approximation, by considering noise at the time samples corresponding to the crossing of the crack by the laser spot. Measurement noise was also considered in the CSLDV signal synthesis, in order to have a Signal to Noise Ratio (SNR) of 30dB. Figure 4 reports the synthesized CSLDV signal and its spectrum for an area scan over the plate surface. The crack scenario addressed in Figure 4 refers to  $\xi_c=1$ .

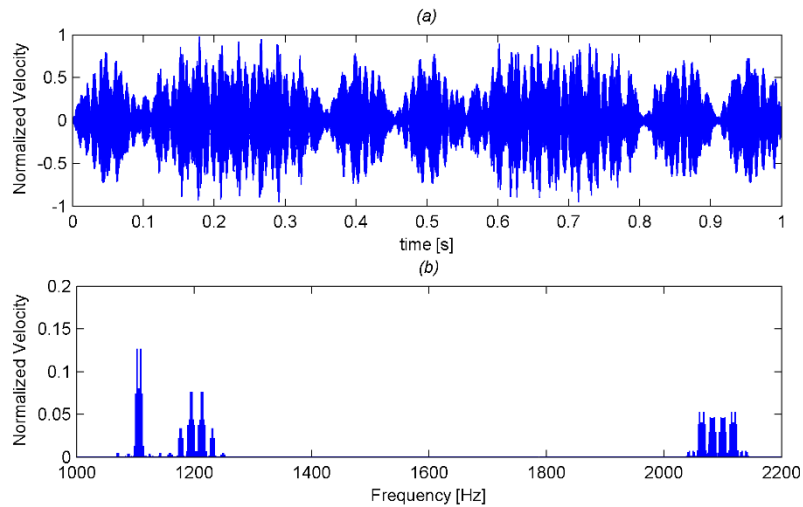


**Figure 4** Synthesized CSLDV signal for an area scan: (a) time domain representation within the time interval  $0s \div 1s$ ; (b) frequency domain representation within the frequency range  $1kHz \div 2.2kHz$

Figures from 5 to 7 report the processed data of the crack scenarios of Figure 1. The RWE method identified Biorthogonal 3.1 (*bior3.1*) wavelet as the mother-wavelet to be used in the processing, while the ESER criterion picked-up the Discrete Meyer (*dmey*) wavelet. The threshold in the following figures is identified as the black dashed line, while samples above the threshold are pictured as red (in colour version only) markers.

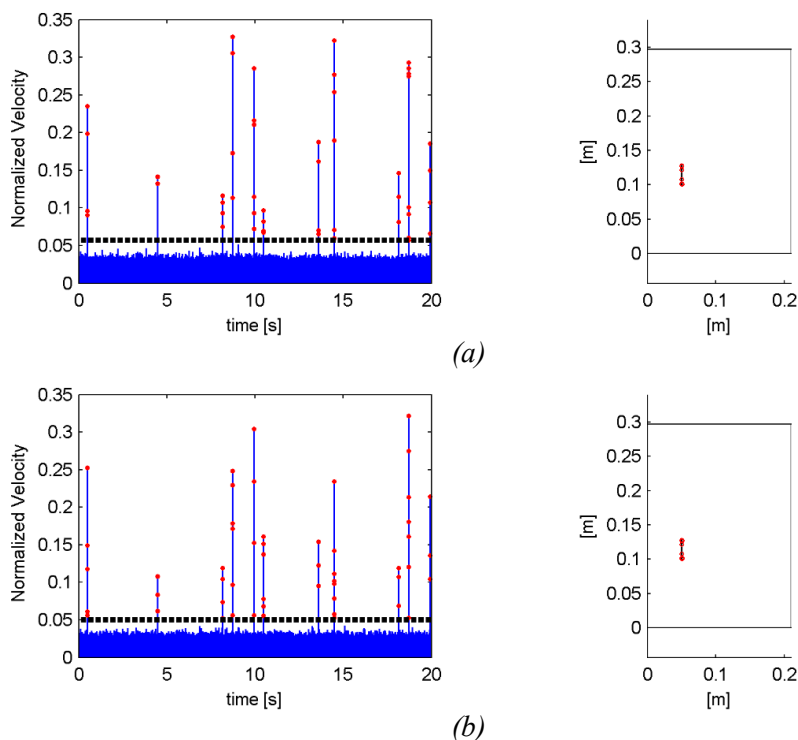


**Figure 5** Crack scenario I: crack depth ratio  $\xi_c=1$  - wavelet selection by RWE (a) and ESER (b) criteria

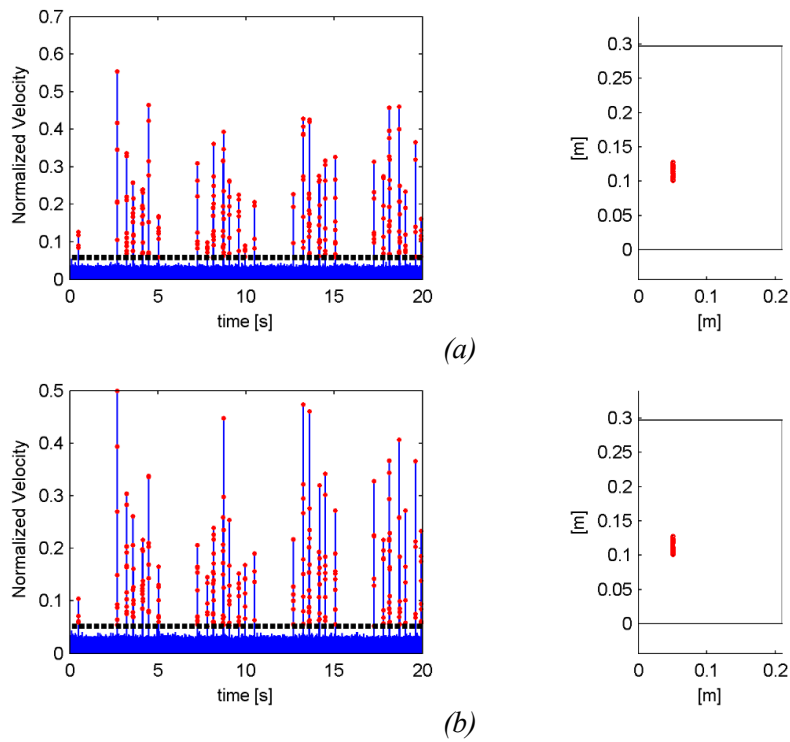


**Figure 6** Crack scenario II: crack depth ratio  $\xi_c=0.5$  – wavelet selection by RWE (a) and ESER (b) criteria

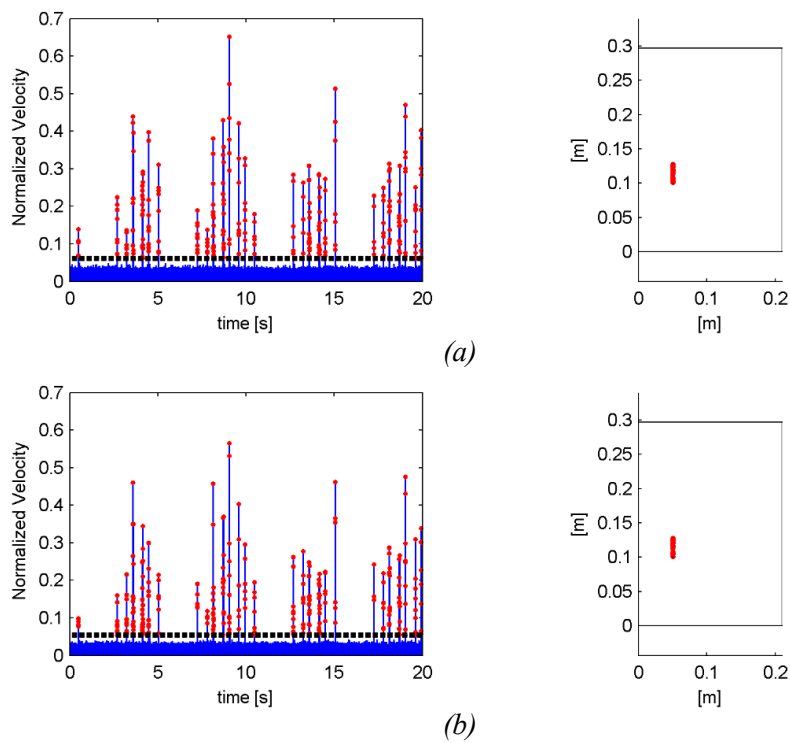


**Figure 7** Crack scenario III: crack depth ratio  $\xi_c=0.25$  – wavelet selection by RWE (a) and ESER (b) criteria



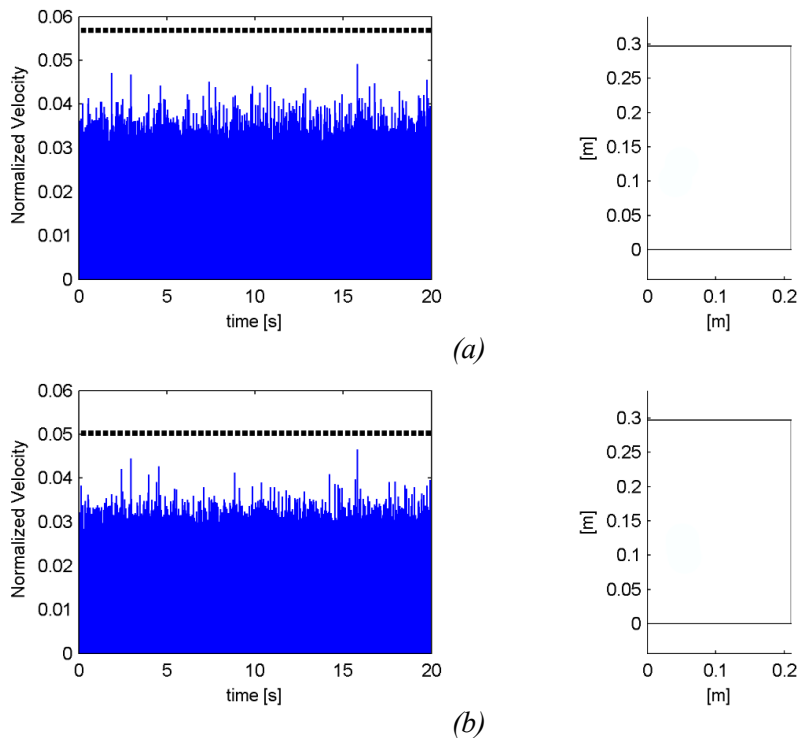


**Figure 8** Damage Detection method on an undamaged plate: wavelet selection by RWE (a) and ESER (b) criteria

The proposed approach is able to identify correctly the cracks in different severity scenarios. No particular differences between results obtained using RWE and ESER criteria for selecting the mother wavelet can be appreciated, despite the two approaches select different wavelets.

The effectiveness of the method can be verified by assessing that no cracks are identified in the undamaged plate. Figure 8 reports results of the application of the approach on such case. No samples are identified above the threshold and therefore no damage is located on the plate.

#### 4. Application of the method on a sub-surface defect

The performances of the method discussed in the previous section were also tested on a virtual experiment reproducing a carbon-fibre composite panel ( $0.210 \times 0.297 \times 0.005$  [m], fibre orientation  $45^\circ$ ) characterized by a damage consisting in an air inclusion of  $0.020 \times 0.020 \times 0.0005$  [m] at a depth of  $0.00025$ m with respect to the panel surface. The geometry of the panel is shown in Figure 9(a).

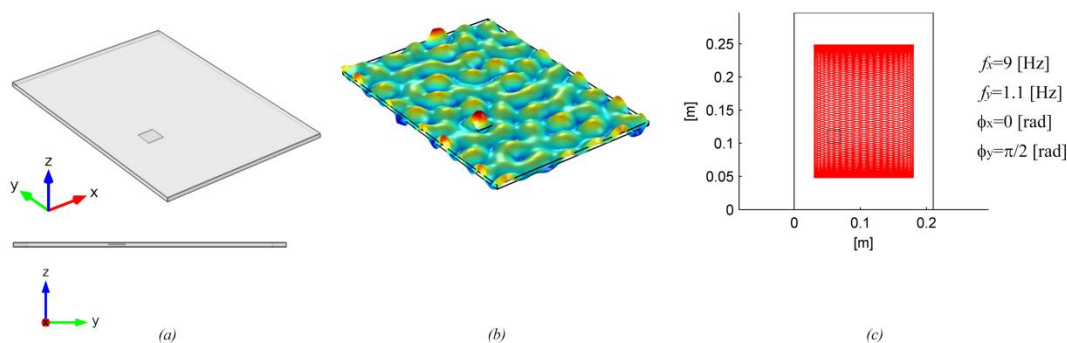


**Figure 9** Virtual experiment on a composite panel: geometry (a); mode shape @ 54189Hz (b); Lissajous pattern used to virtually perform an area scan on the test panel (c)

The CSLDV signal was synthesized using the approach discussed in Section 3, namely using as amplitude-modulating function for the CSLDV vibration signal the mass-normalized mode shape shown in Figure 9(b). The choice to work on such high frequency range was due to the need of avoiding contributions due to high-energy global modes (low frequency modes). Measurement noise was added to the CSLDV synthesized signal in order to have a SNR of 30dB. The scan pattern used was the Lissajous pattern reported in Figure 9(c), where the relative defect-laser path orientation is also shown. Sampling frequency was set to 200kHz, for a record length of 10s.

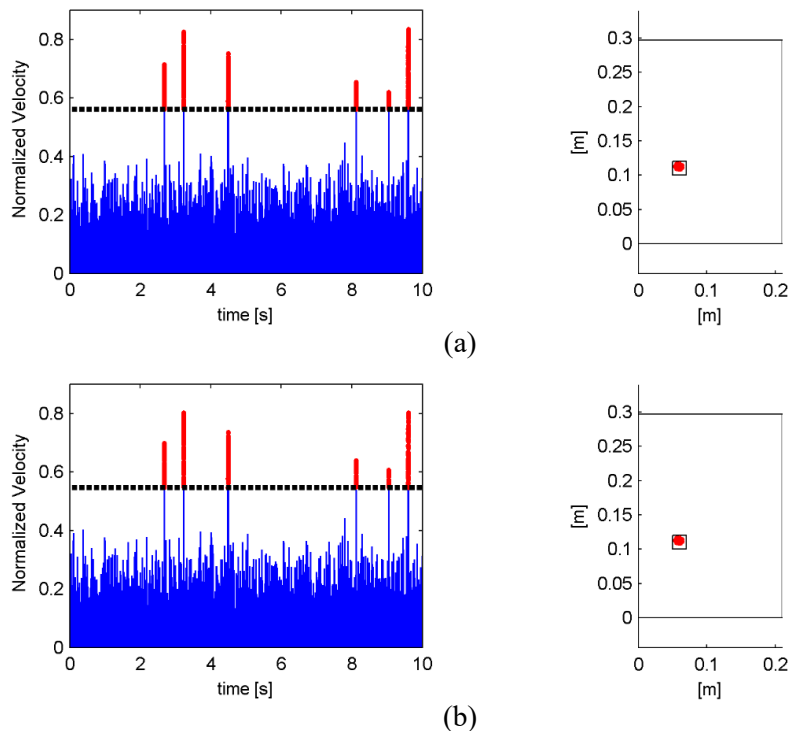


**Figure 10** Sub-surface defect on a carbon-fibre composite panel: results of CSLDV and wavelet-processing – wavelet selection by RWE (a) and ESER (b) criteria

The RWE criterion identified Biorthogonal 3.9 (*bior3.9*) as mother-wavelet for CSLDV processing, while the ESER criterion identified the Reversed Biorthogonal 3.9 (*rbior3.9*) wavelet. The Details of wavelet decompositions at level 3 contain the information associated to the presence of the defect. Indeed by applying the thresholding method of (1) the spatial position of the defect can be well localized, as reported in Figure 10. Again the two criteria for selecting the mother wavelet do imply similar results on CSLDV signal decomposition and on damage detection capability. As in previous figures reporting processing results, the threshold is identified as the black dashed line, while samples above the threshold are pictured as red (in colour version only) markers.

### 5. Application of the method on a real test case

The approach presented in the previous sections was also applied on a real test case. The sample under test is a steel plate ( $0.200 \times 0.290 \times 0.002$  [m]) with several through-cracks. Figure 11 reports the plate examined together with the specifications of the defect under analysis and CSLDV scanning area.

In order to verify the approach on a real case scenario the test was performed over an area that comprises defect #1 only. White noise in the range  $2\text{kHz} \div 100\text{kHz}$  drove a piezo exciter located on the top-left corner of the clamped-free plate.

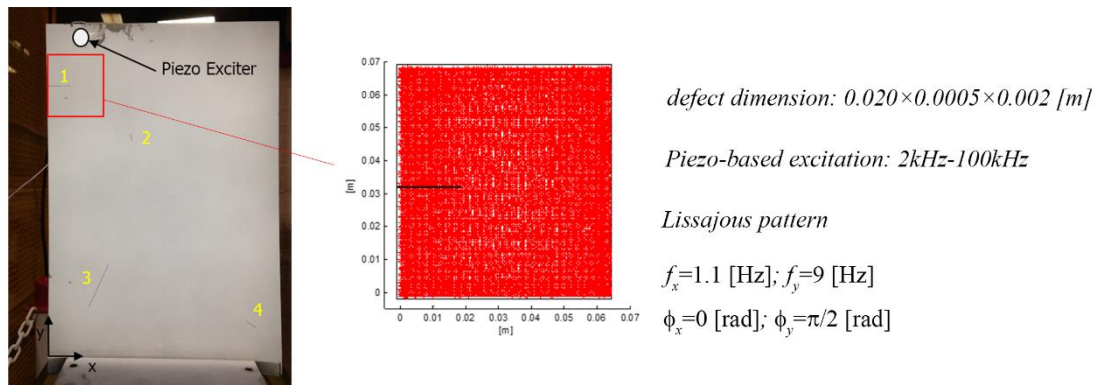


**Figure 11** Steel plate under test and area scan performed over defect #1

The method was applied using both Relative Wavelet Energy and Energy to Shannon Entropy Ratio criteria to choose the mother-wavelet. The first identified *Haar* wavelet as mother-wavelet, while the latter criterion the Reverse Biorthogonal 3.1 (*rbio3.1*) wavelet.

**Table 2** Frequency Ranges corresponding to nodes from Wavelet Packet Decomposition Tree

Node number	Frequency Range [kHz]
6	75.00 – 100.00
14	87.50 – 100.00
30	93.75 – 100.00

Figures 12, 13 and 14 report results from the use of the defect detection approach proposed at different nodes of the decomposition tree. Such nodes are those referring to, respectively, frequency ranges reported in Table 2.

Defect is generally well identified by the method, even though some spots out of the damaged region are recognized as possible defects locations. Nevertheless, it is interesting to notice that spatial samples in the crack region are always located in the same position, while the latter are randomly distributed within all the decomposition nodes. This phenomenon suggests that further processing can be made on the spatial distribution of the points, in order to separate those that refer to the crack from those that are false-positives. Authors are currently studying different approaches to better isolate the defect region and to make the final map containing only the damage. *Haar* and *rbio3.1* wavelets give almost similar results. However, it is worth noticing that *rbior3.1* seems better locating the crack all over its extension, while *Haar* produces maps with less false-positives, even though the length of the defect is misidentified at higher nodes (14 and 30). Apparently, the RWE method works better than ESER when the decomposition node extends to low-frequency (node 6).

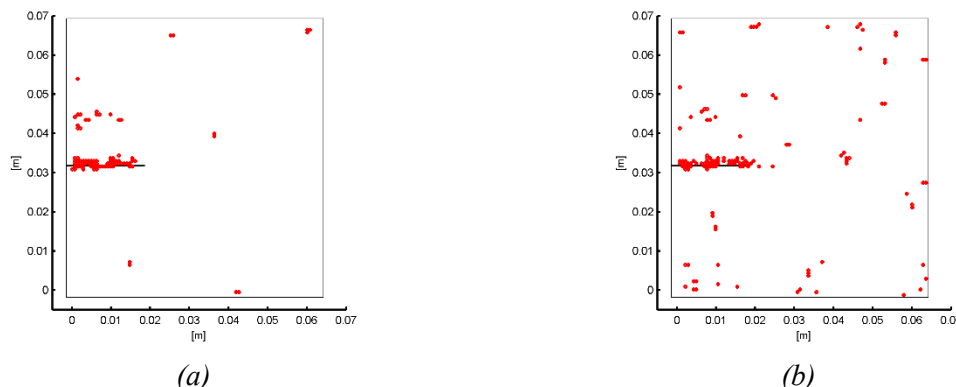


**Figure 12** Decomposition at node #6: RWE (a) and Energy to Shannon Entropy Ratio (b) criteria

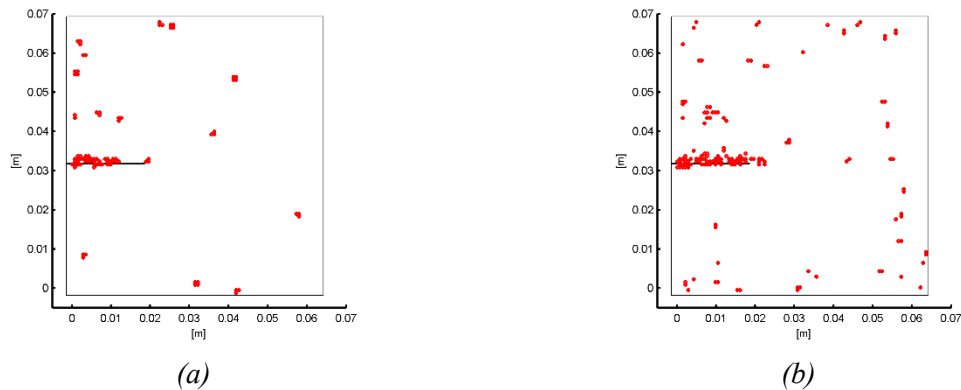


**Figure 13** Decomposition at node #14: RWE (a) and Energy to Shannon Entropy Ratio (b) criteria

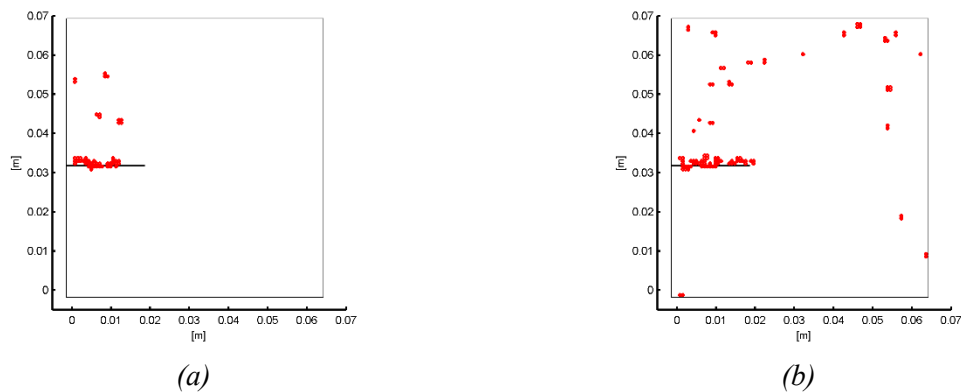


**Figure 14** Decomposition at node #30: RWE (a) and Energy to Shannon Entropy Ratio (b) criteria

## 6. Conclusions

The paper presented and discussed an evolution of a damage detection approach, which was already presented by the authors, based on CSLDV and wavelet-processing. CSLDV is highly sensitive to shape discontinuities, mainly because its inherent characteristic of giving as output a signal that is amplitude modulated by the mode shapes of the structure. Moreover, the deformation gradient that takes place in superficial damages as cracks produces a further discontinuity in the time signal that is linked to the interaction of laser light with the defect edges. Dealing with a technique, as CSLDV is, that shows an almost infinite spatial resolution increase the possibility of crossing the damage and then in locating it. The processing based on wavelet decomposition has resulted efficient in identifying these discontinuities, especially if used together with a thresholding approach based on the combined use of SURE criterion and the RMS of the signal extracted from the wavelet decomposition. With respect to the damage detection strategy presented by authors in a previous work, two procedures for selecting the mother-wavelet in an objective manner have been proposed and compared, the Relative Wavelet Energy and the Energy to Shannon Entropy Ratio, in this paper. The focus has also been put on the area scan testing procedure: such scanning method represents the only possible approach to target real applications, since defects location is never known a-priori.

The procedure was tested on a simulated test case for different crack scenarios (varying crack depth ratio). The method showed promising results, since cracks were identified in all severity conditions. An application on a sub-surface scenario for a carbon-fibre composite panel was discussed as well. Again, the method was able to localize the defect with good accuracy.

Preliminary results from the application of the approach on a real test case were also discussed. The defect, a through- crack on a steel plate, is well identified by the algorithm proposed by the authors, even though some false-positives (spatial samples labelled as damages even if no damages are present)

rise. Authors are currently working in developing a methodology to isolate better the damaged areas in real test cases.

Finally, it is important to stress out the main advantage of the defect identification method proposed by the authors: with respect to previously proposed approaches, the one addressed by the authors does not need any analysis on the mode shapes of the structure, neither any foreknowledge of the undamaged structure. This is for sure a key element that makes the method linked to the nature of the defect rather than to the structure itself. Last but not least, authors are trying to set-up a procedure that does not require any decision of the end-user regarding parameters to be set (e.g. threshold, mother-wavelet-selection). This is also an important aspect to be taken into account in a damage detection approach, since damage identification should be performed in a way as much objective as possible in order to avoid any possibility of misunderstanding result.

## References

- [1] Castellini P, Revel G M, Tomasini E P 1998 Laser Doppler Vibrometry: a review of advances and applications *The Shock And Vibration Digest* **30**(6) pp 443-456
- [2] Di Sante R, Revel G M, Rossi G L 2000 Measurement techniques for the acoustic analysis of synchronous belts *Measurement Science and Technology* **11** 10 pp 1463-1472
- [3] Revel G M, Martarelli M, Chiariotti P 2010 A new laser vibrometry-based 2D selective intensity method for source identification in reverberant fields: Part I. Development of the technique and preliminary validation *Measurement Science and Technology* **21** 7 075107
- [4] Marchionni P, Scalise L, Ercoli I, Tomasini E P 2013 An optical measurement method for the simultaneous assessment of respiration and heart rates in preterm infants *Review Of Scientific Instruments American Institute Of Physics* **84** 121705
- [5] Castellini P, Revel G M 2000 Laser vibration measurements and data processing for structural diagnostic on composite materials *Review Of Scientific Instruments American Institute Of Physics* **7** pp 207-215
- [6] Stanbridge A B, Martarelli M, Ewins D J 2004 Measuring area vibration mode shapes with a continuous-scan LDV *Measurement* **35** 2 pp 181-189
- [7] Chiariotti P, Martarelli M, Revel G M 2014 Exploiting continuous scanning laser Doppler vibrometry (CSLDV) in time domain correlation methods for noise source identification, *Measurement Science and Technology*, **25**(7) 075204 doi: 10.1088/0957-0233/25/7/075204
- [8] Stanbridge A B, Khan A Z, Ewins D J 1997 Fault identification in vibrating structures using a scanning laser doppler vibrometer, *Proceedings of the International Workshop on Structural Health Monitoring (Stanford, CA, USA, September 18-20)* pp 56-65
- [9] Khan A Z, Stanbridge A B, Ewins D J 2000 Detecting damage in vibrating structures with a scanning LDV *Optics and Lasers in Engineering* **32** pp 583-592
- [10] Chukwujekwu Okafor A, Dutta A 2000 Structural damage detection in beams by wavelet transforms *Smart Materials and Structures* **9** 6 doi:10.1088/0964-1726/9/6/323
- [11] Kim H, Melhem H 2004 Damage detection of structures by wavelet analysis *Engineering Structures* **26** pp 347-362
- [12] Radziński M, Krawczuk M 2009 Experimental verification and comparison of mode shape-based damage detection methods *Journal of Physics: Conference Series* **181** 012067 doi:10.1088/1742-6596/181/1/012067
- [13] Cao M, Xu W, Ostachowicz W, Zhongqing S 2014 Damage identification for beams in noisy conditions based on Teager energy operator-wavelet transform modal curvature *Journal of Sound and Vibration* **333** 6 pp 1543-1533
- [14] Chiariotti P, Revel G M, Martarelli M 2015 Exploiting Continuous Scanning Laser Doppler Vibrometry and Wavelet Processing for Damage Detection *Experimental Techniques, Rotating Machinery, and Acoustics Conference Proceedings of the Society for Experimental Mechanics Series* **8** pp 189-196 doi: 10.1007/978-3-319-15236-3\_18
- [15] Martarelli M, Ewins D J 2006 Continuous scanning laser Doppler vibrometry and speckle noise

- occurrence *Mechanical Systems and Signal Processing* **20** 8 pp 2277–2289
- [16] Salto N 2004 Simultaneous noise suppression and signal compression using a library of orthonormal bases and the minimum description length criterion, In: (2nd ed.), E. Foufoula-Georgiou and P. Kumar, Editors, *Wavelets in Geophysics*, Academic Press. (2004).
- [17] Yan R 2007 Base wavelet selection criteria for non-stationary vibration analysis in bearing health diagnosis *Electronic Doctoral Dissertations for UMass Amherst* Paper AAI3275786, <http://scholarworks.umass.edu/dissertations/AAI3275786>, January 1, 2007
- [18] Rafiee J and Tse P W 2009 Use of autocorrelation of wavelet coefficients for fault diagnosis *Mechanical System and Signal Processing* **23** 5 pp 1554-1572
- [19] Ngui W K, Leong M S, Hee L M, Abdelrhman A M 2013 Wavelet Analysis: Mother Wavelet Selection Methods *Applied Mechanics and Materials* **393** pp 953-958
- [20] Kankar P K, Sharma S C, Harsha S P 2011 Fault diagnosis of ball bearings using continuous wavelet transform *Applied Soft Computing* **11** 2 pp 2300-2312 <http://dx.doi.org/10.1016/j.asoc.2010.08.011>.
- [21] Donoho D L, Johnstone I M 1995 Adapting to unknown smoothness via wavelet shrinkage *Journal of the American Statistical Association* **90** pp 1200-1224